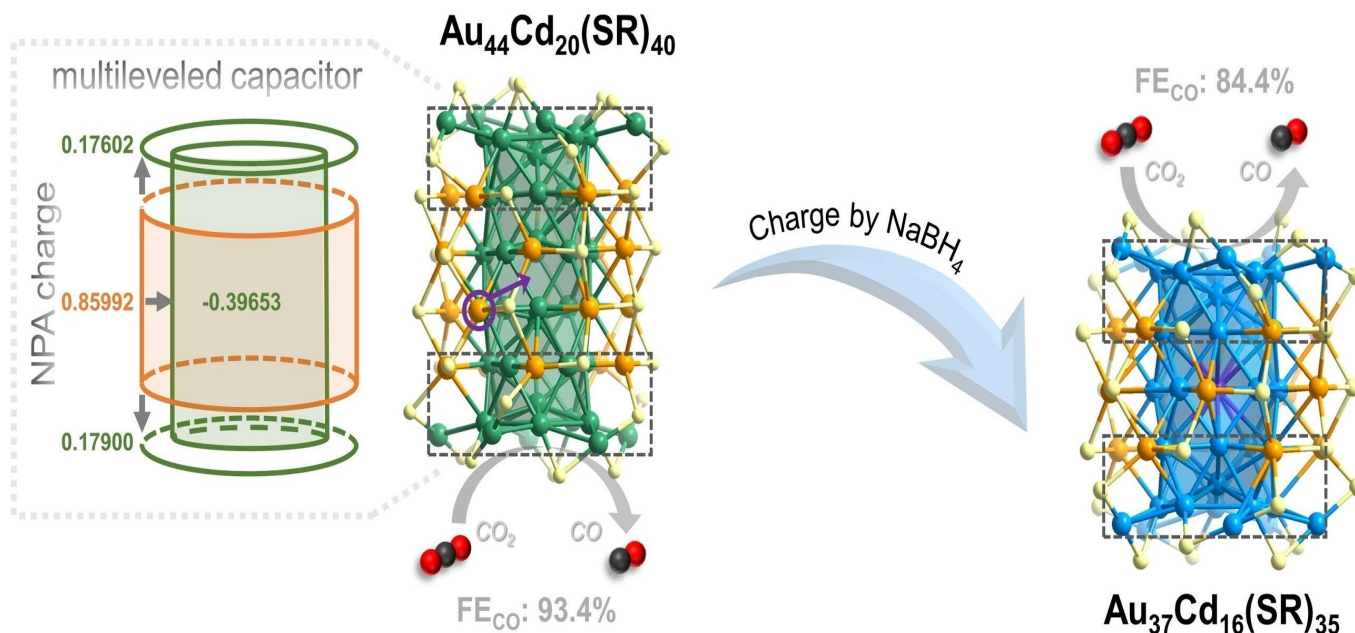


# Chemical Synthesis of ~1 nm Multilevel Capacitor-like Particles with Atomic Precision

Yue Zhou<sup>+</sup>, Dong Chen<sup>+</sup>, Wanmiao Gu<sup>+</sup>, Wentao Fan<sup>+</sup>, Runguo Wang, Liang Fang, Qing You, Shengli Zhuang, Guoqing Bian, Lingwen Liao, Ziyang Zhou, Nan Xia,<sup>\*</sup> Jun Yang,<sup>\*</sup> and Zhikun Wu<sup>\*</sup>



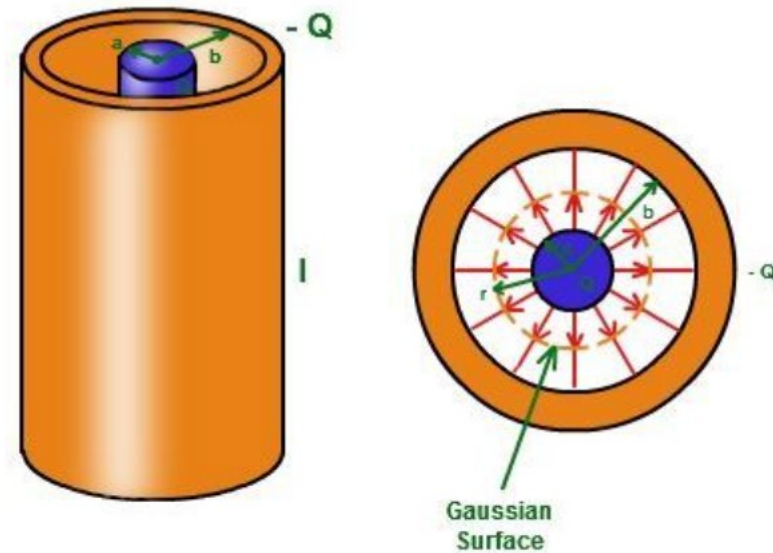
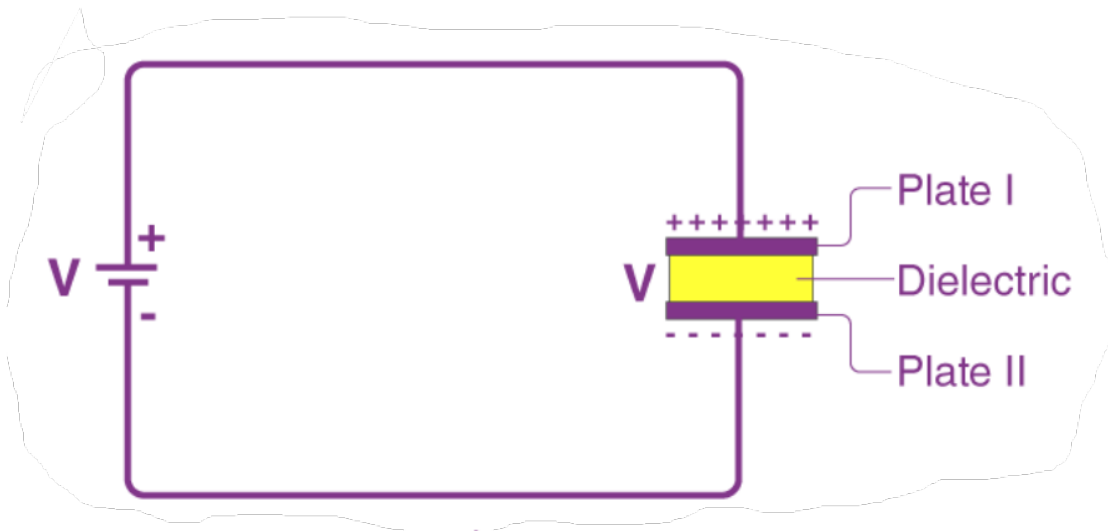
Publication date:  
2<sup>nd</sup> December 2024

Paper Presentation

Sooraj B S  
28-12-2024

# Capacitor

- Capacitors are energy-storing devices available in different shapes and sizes
- It is made up of two conducting plates separated by an insulating material called a dielectric
- It can undergo charging and discharging



### Cylindrical Capacitor

# Motivation

- Emerging metal nanoclusters have atomically precise and tunable compositions and structures, facilitating the fabrication of ultrasmall nanosized devices
- Some NCs have core-shell or multiple-shell metal structures
- It is essential to verify whether such a core-shell or multiple-shell structure can function as an ultrasmall capacitor (Nanocluster capacitor)
- However, techniques to identify the charging and discharging process of NC capacitor, is not achieved yet
- To address these requirements, the latter one, we realized the synthesis of challenging Au core-Cd shell bimetal NCs, considering that the two metals have a large electronegativity difference

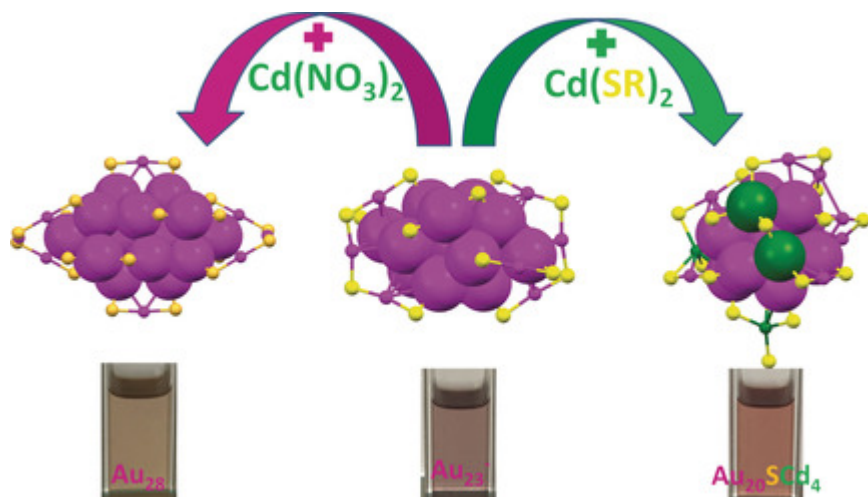
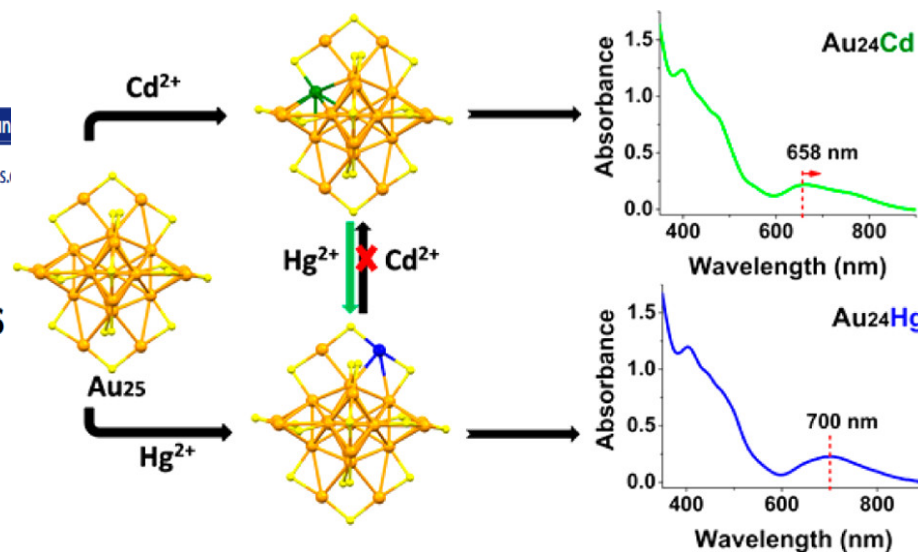
# Background Work



Commun  
pubs.acs.org

## Mono-cadmium vs Mono-mercury Doping of $\text{Au}_{25}$ Nanoclusters

Chuanhao Yao,<sup>†,§</sup> Yue-jian Lin,<sup>‡,§</sup> Jinyun Yuan,<sup>||,§</sup> Lingwen Liao,<sup>†</sup> Min Zhu,<sup>†</sup> Lin-hong Weng,<sup>\*,‡</sup>  
Jinlong Yang,<sup>\*,||</sup> and Zhikun Wu<sup>\*,†</sup>



Communications



Nanoparticles

International Edition: DOI: 10.1002/anie.201800877  
German Edition: DOI: 10.1002/ange.201800877

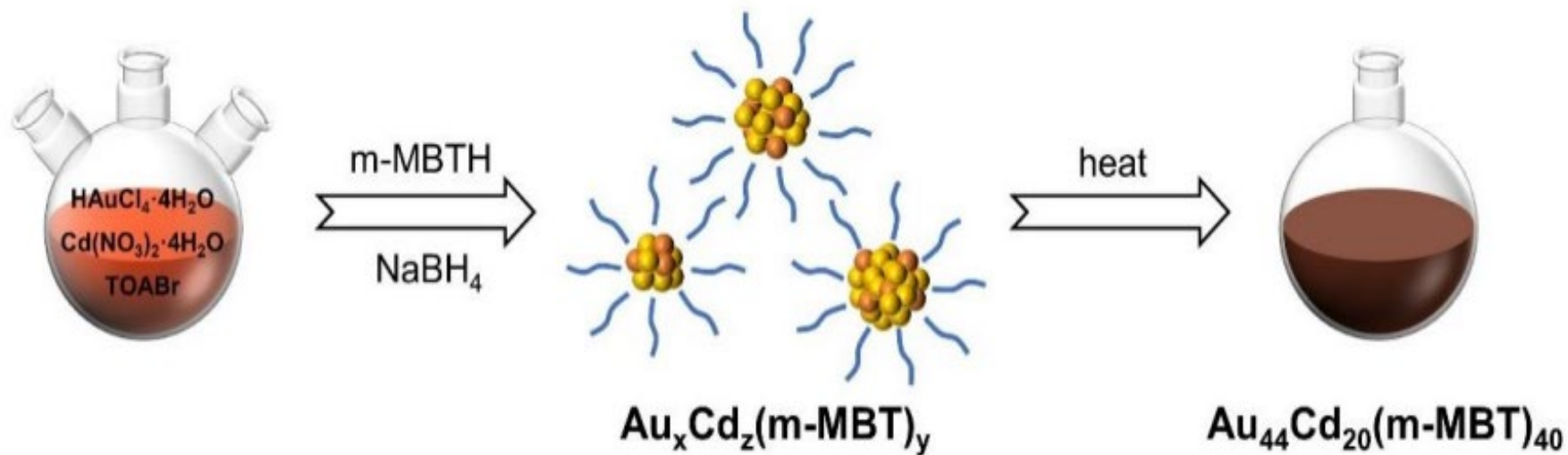
## The Fourth Alloying Mode by Way of Anti-Galvanic Reaction

Min Zhu<sup>†</sup>, Pu Wang<sup>†</sup>, Nan Yan<sup>†</sup>, Xiaoqi Chai, Lizhong He, Yan Zhao, Nan Xia,  
Chuanhao Yao, Jin Li, Haiteng Deng, Yan Zhu, Yong Pei,<sup>\*</sup> and Zhikun Wu<sup>\*</sup>

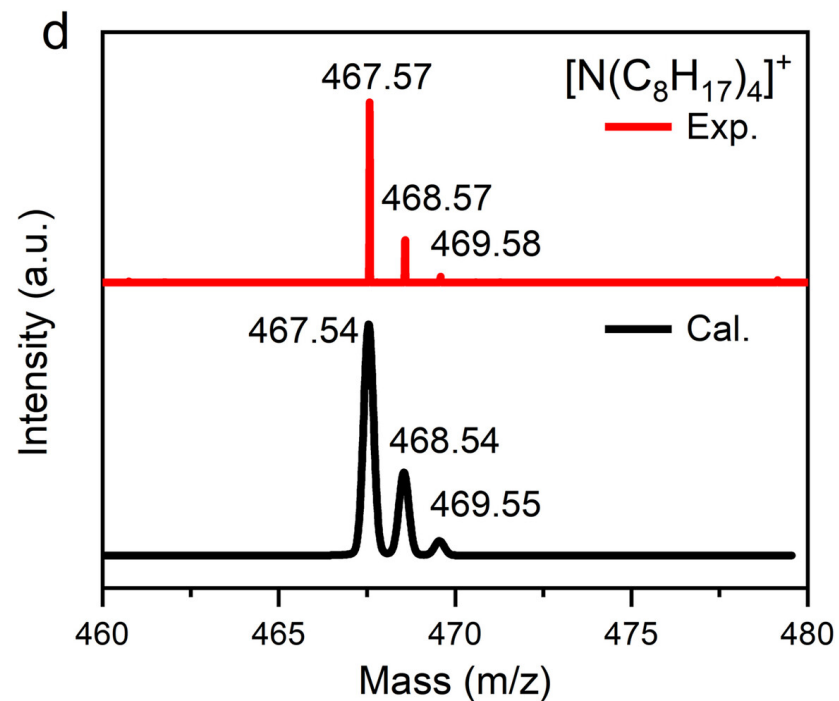
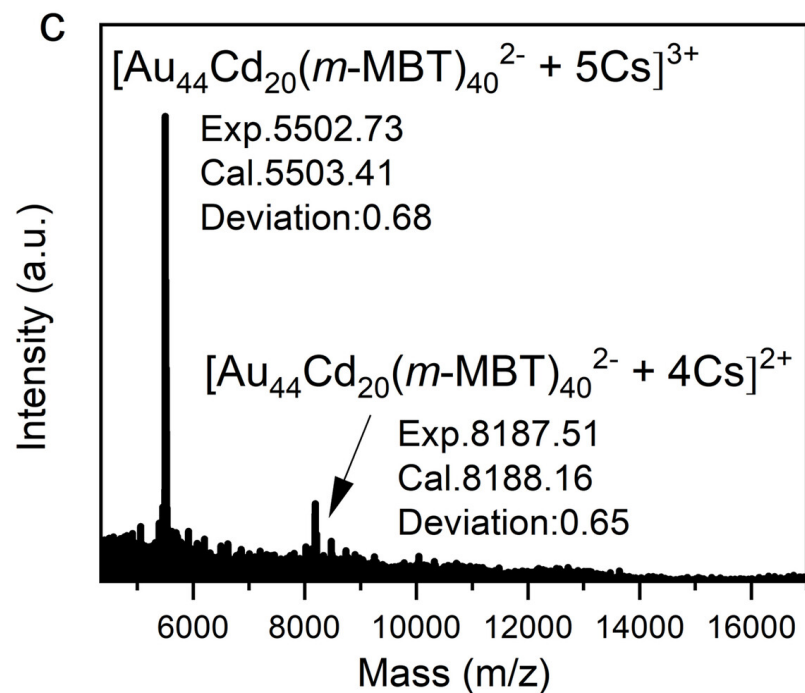
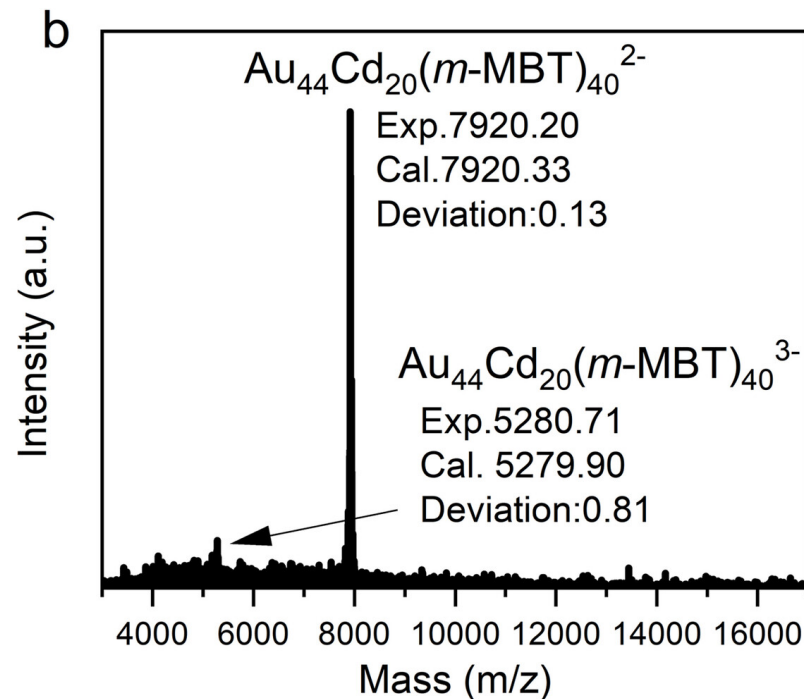
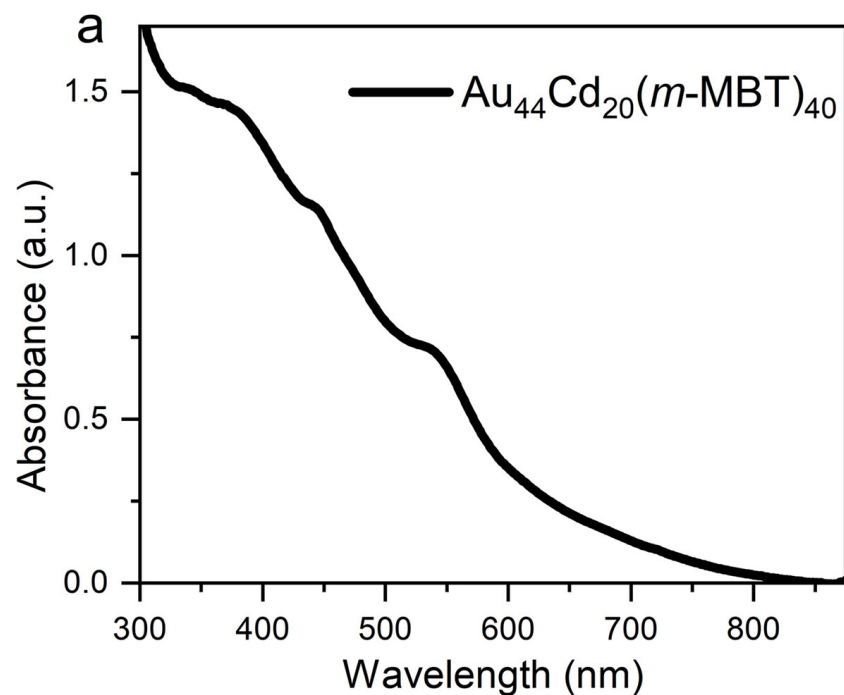
# Why this paper

- First report on the feasibility of the application of metal nanoclusters as multilevel capacitors with atomic precision
- First report on the intra-nanoparticle charge movement and the intra-nanocluster anti-galvanic reaction by undoubted single crystal X-ray diffraction
- First report on central atom Cd doping of bimetallic nanoclusters

# This work



**Figure S1.** The synthesis route.





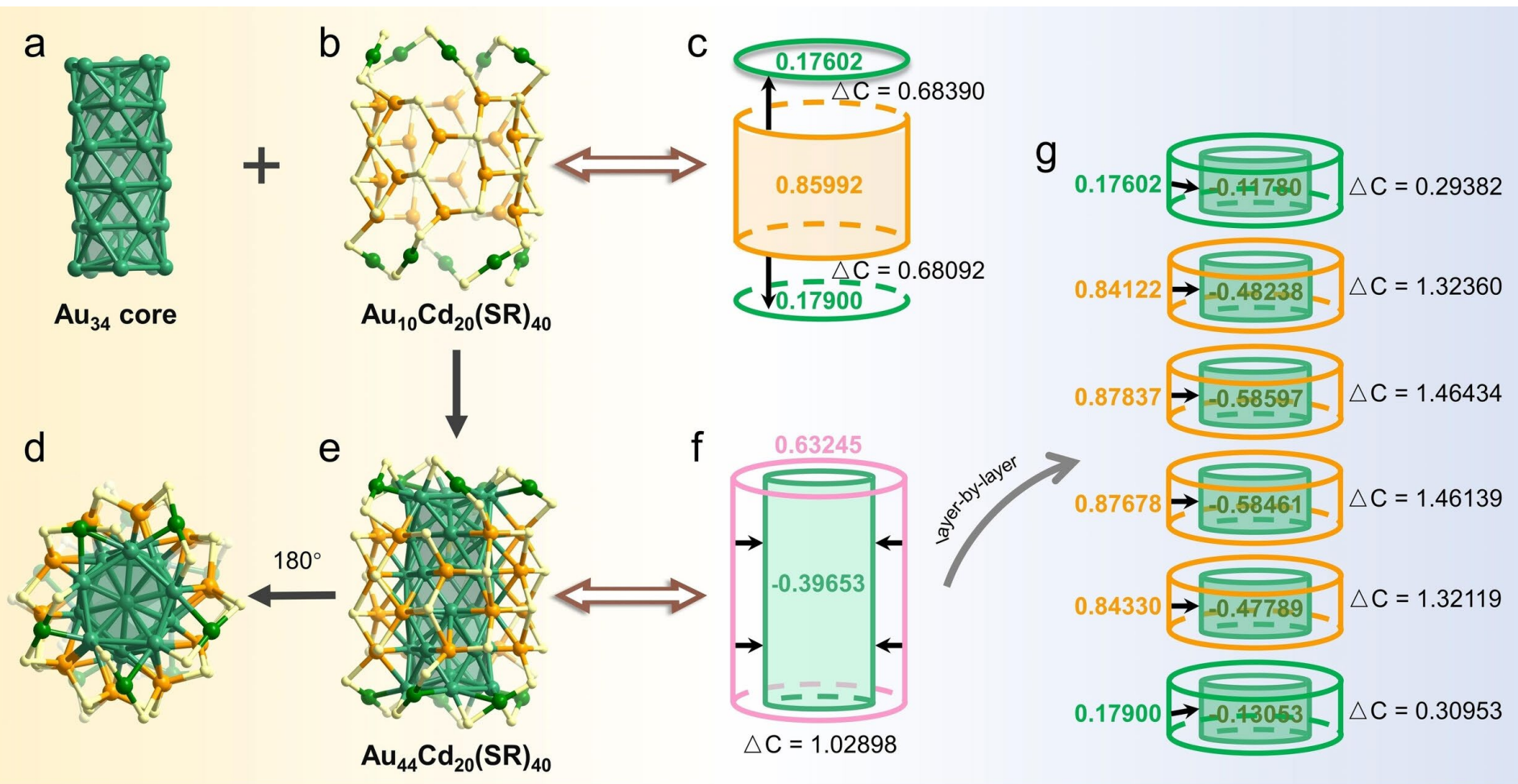


**Figure 1.** Structure anatomy and illustration of multilevel capacitor of  $\text{Au}_{44}\text{Cd}_{20}$ . (a)  $\text{Au}_{34}$  core. (b)  $\text{Au}_{10}\text{Cd}_{20}(\text{SR})_{40}$  staple. (c) Average NPA charge differences ( $\Delta C$ ) between Au and Cd sections in the shell. (d) Top and (e) side views of the complete structure. (f) Average NPA charge differences between the AuCd shell and Au core. (g) Average NPA charge differences between the  $\text{Cd}_5$  ( $\text{Au}_5$ ) shell pentagon and the corresponding  $\text{Au}_5$  core pentagon. Carbon and hydrogen atoms are omitted for clarity. Cd: orange, S: yellow, and Au: other color.



a



Pentagonal  
bipyramid  $\text{Au}_7$

+



pentagonal  
antiprisms  $\text{Au}_{10}$

+



Pentagonal  
bipyramid  $\text{Au}_7$

+



Pentagonal  $\text{Au}_5$  at  
the top and bottom

=



$\text{Au}_{34}$  core

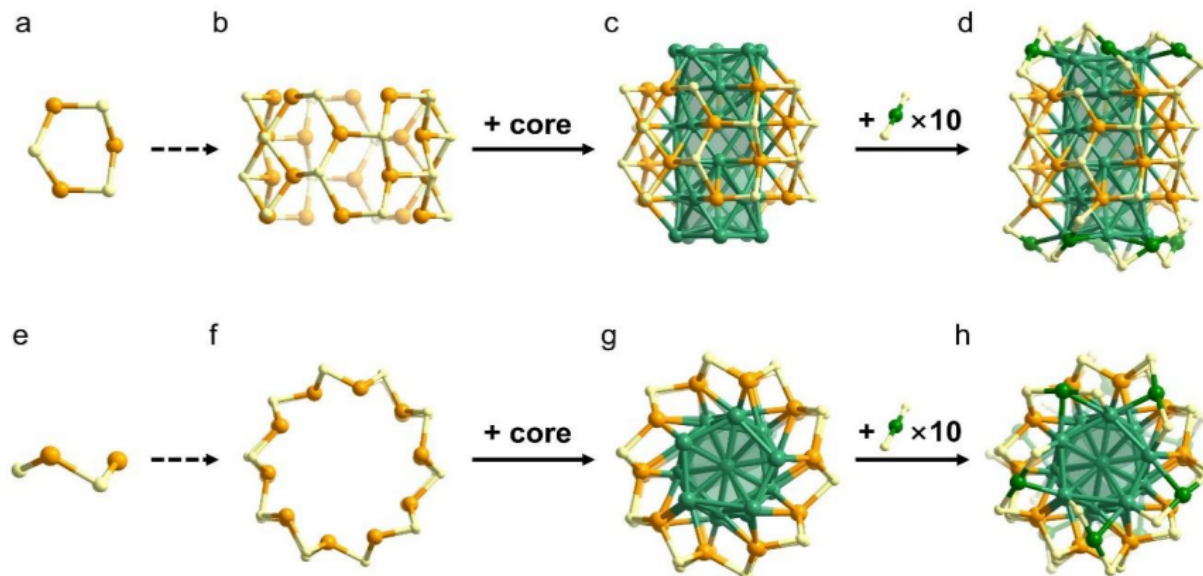


**Figure S4.** Anatomy of the structure of the  $\text{Au}_{44}\text{Cd}_{20}$ . (a, e) Starting from the motif of  $\text{Cd}_3(\text{m-MBT})_3$ ; (b, f) the motif of  $\text{Cd}_{20}(\text{m-MBT})_{20}$ ; (c, g) adding the core to form the  $\text{Au}_{34}\text{Cd}_{20}(\text{m-MBT})_{20}$  framework; and (d, h) finally adding ten  $\text{Au}(\text{m-MBT})_2$  unit to form the complete structure of  $\text{Au}_{44}\text{Cd}_{20}(\text{m-MBT})_{40}$ . Side view: a-d; top view: e-h. For clarity, C and H atoms are all omitted. Cd, orange; S, yellow; Au, other color.

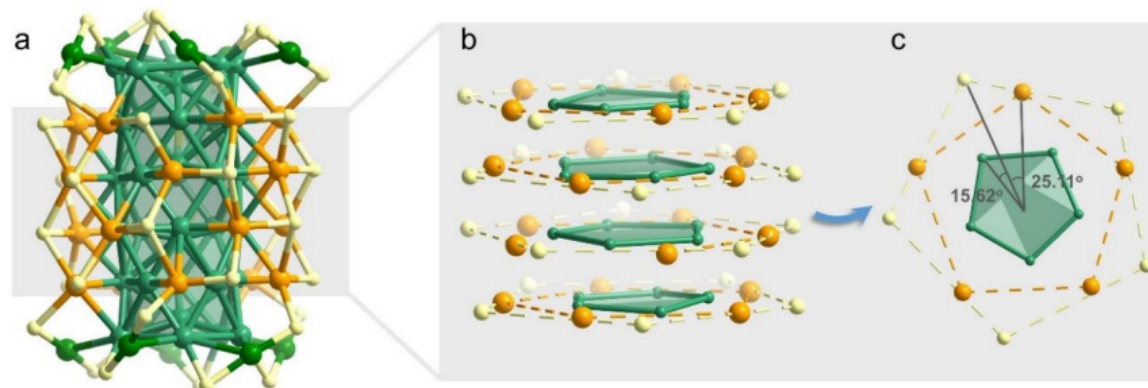


**Figure S5.** Layer by layer atomic arrangement of  $\text{Au}_{44}\text{Cd}_{20}$ . (a) Structure of  $\text{Au}_{44}\text{Cd}_{20}$ . (b) Illustration of  $\text{S}_5$ ,  $\text{Cd}_5$ , and  $\text{Au}_5$  pentagons in  $\text{Au}_{44}\text{Cd}_{20}$ . (c) Rotation relation between  $\text{S}_5$ ,  $\text{Cd}_5$ , and  $\text{Au}_5$  pentagons in the same layer of  $\text{Au}_{44}\text{Cd}_{20}$ . For clarity, C and H atoms are all omitted. Cd, orange; S, yellow; Au, other color.

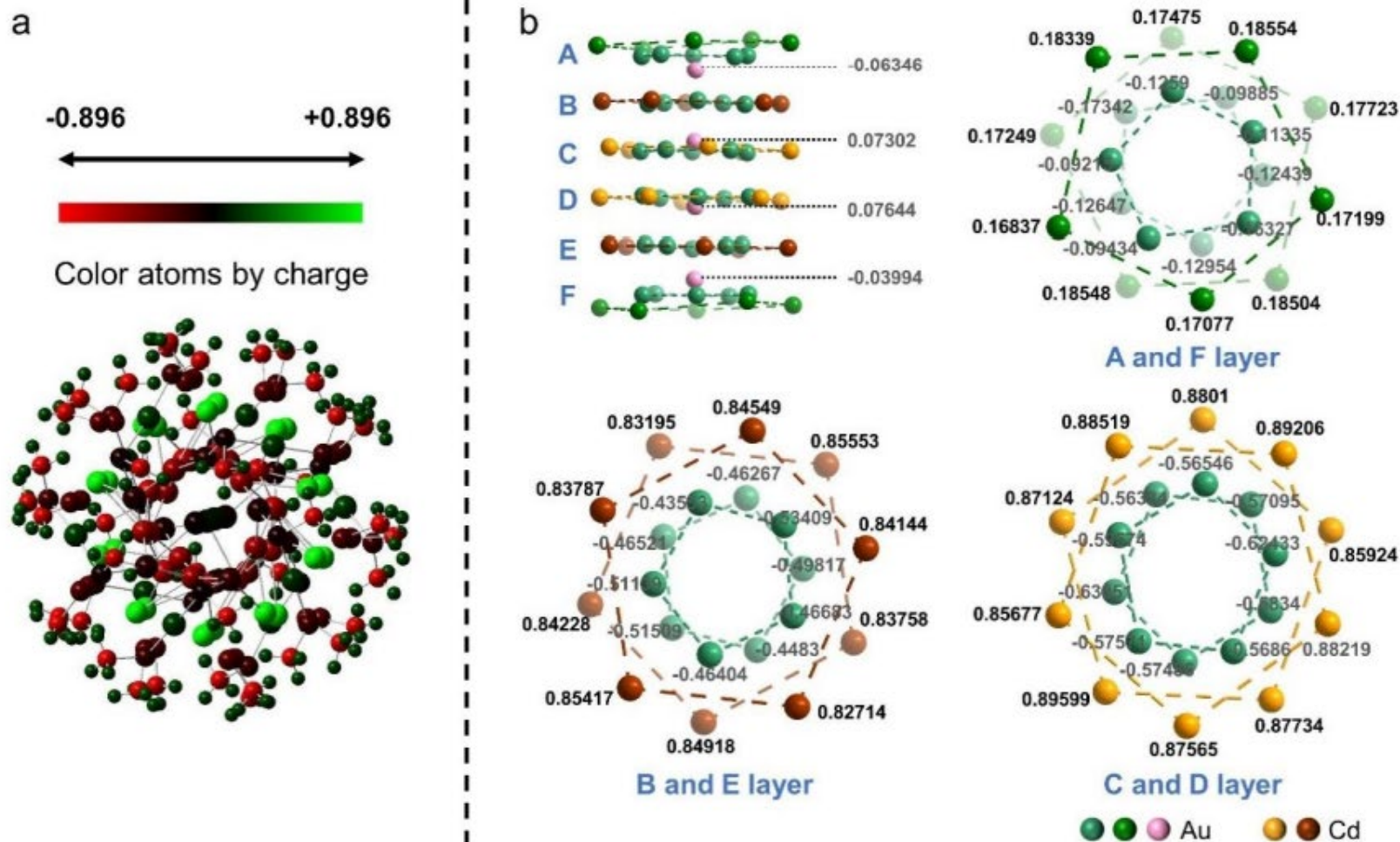


**Figure S6.** NPA charge distribution of  $\text{Au}_{44}\text{Cd}_{20}$ . For clarity, all C and H atoms are omitted.



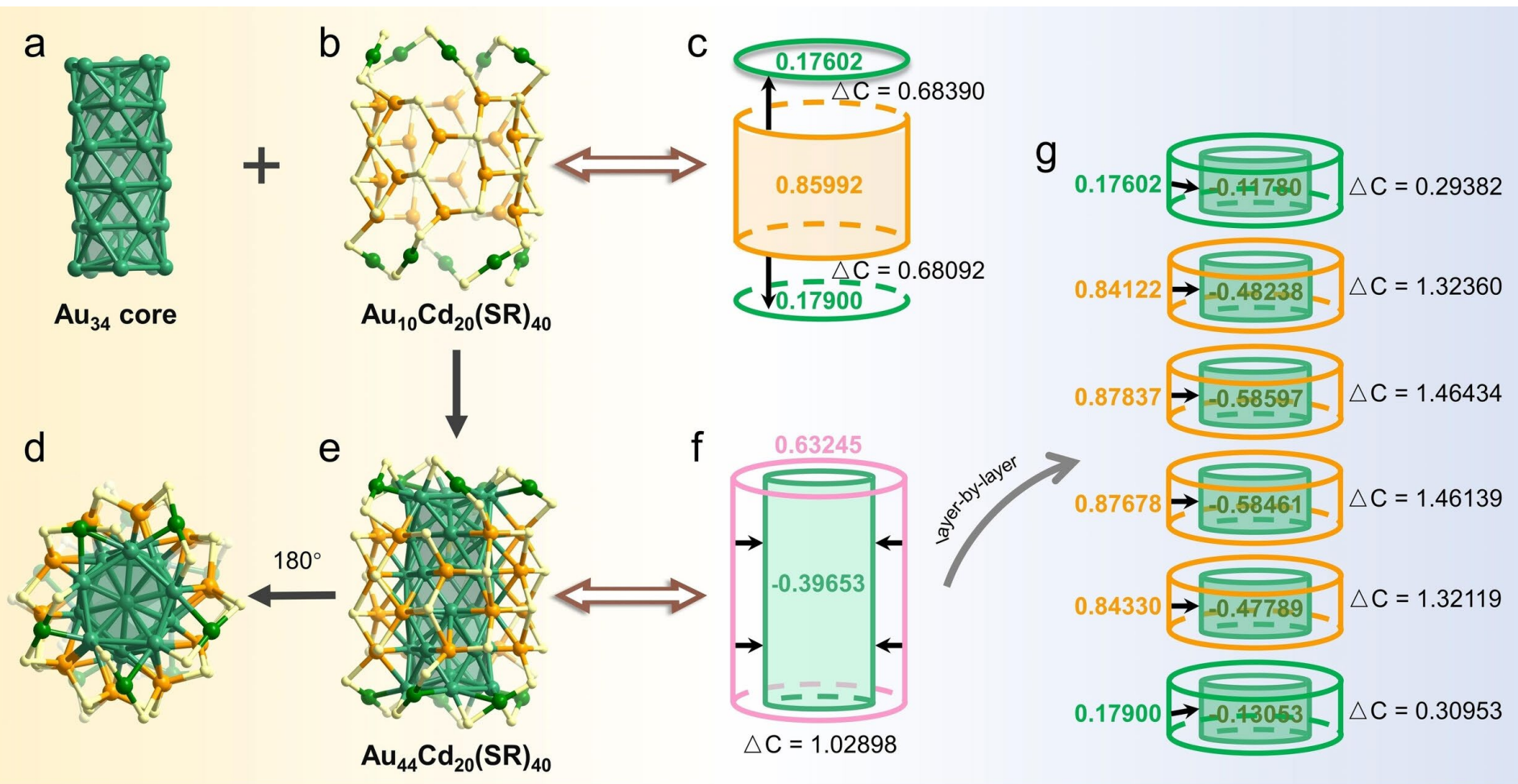


**Figure 1.** Structure anatomy and illustration of multilevel capacitor of  $\text{Au}_{44}\text{Cd}_{20}$ . (a)  $\text{Au}_{34}$  core. (b)  $\text{Au}_{10}\text{Cd}_{20}(\text{SR})_{40}$  staple. (c) Average NPA charge differences ( $\Delta C$ ) between Au and Cd sections in the shell. (d) Top and (e) side views of the complete structure. (f) Average NPA charge differences between the AuCd shell and Au core. (g) Average NPA charge differences between the  $\text{Cd}_5$  ( $\text{Au}_5$ ) shell pentagon and the corresponding  $\text{Au}_5$  core pentagon. Carbon and hydrogen atoms are omitted for clarity. Cd: orange, S: yellow, and Au: other color.

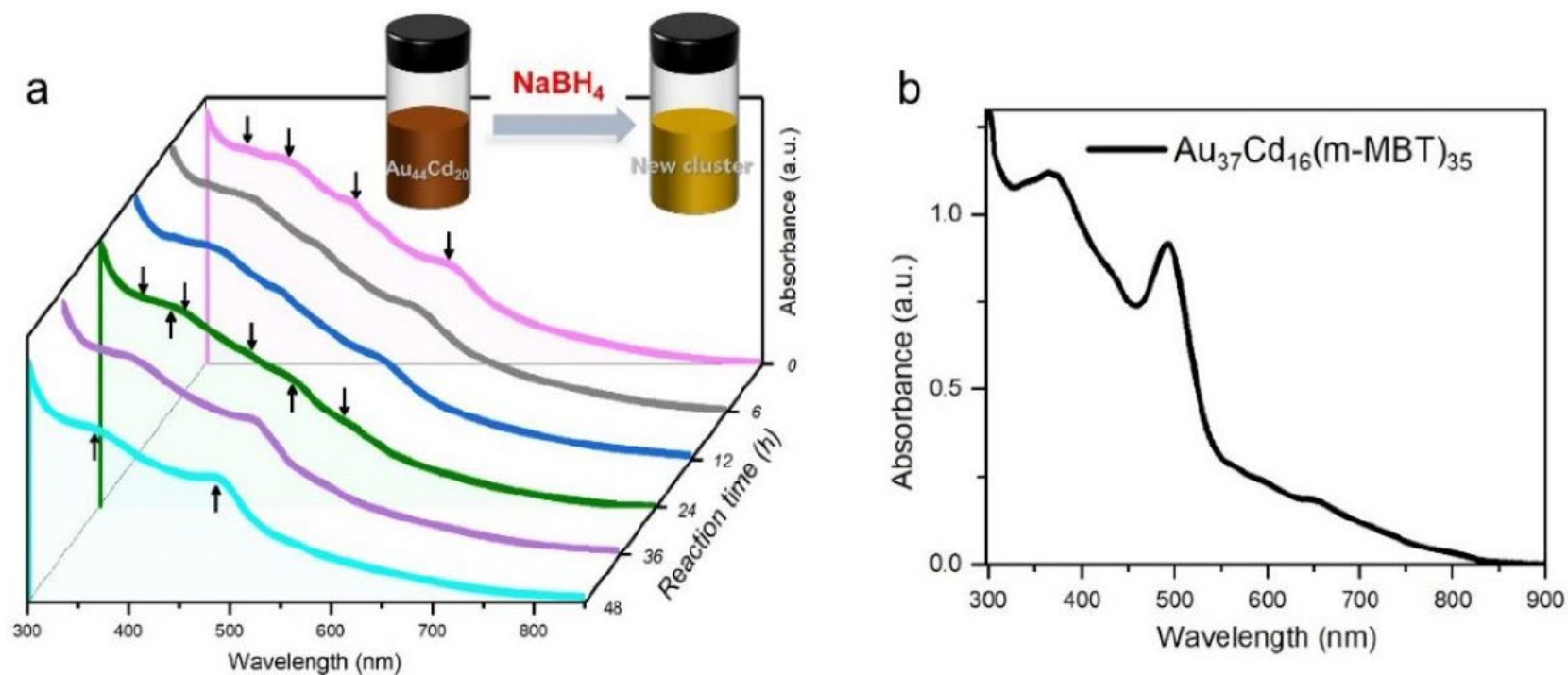


**Figure S7.** (a) UV/vis/NIR absorption spectrum of  $\text{Au}_{44}\text{Cd}_{20}$  charged by  $\text{NaBH}_4$  at different times. (b) UV/vis/NIR absorption spectrum of  $\text{Au}_{37}\text{Cd}_{16}$ .

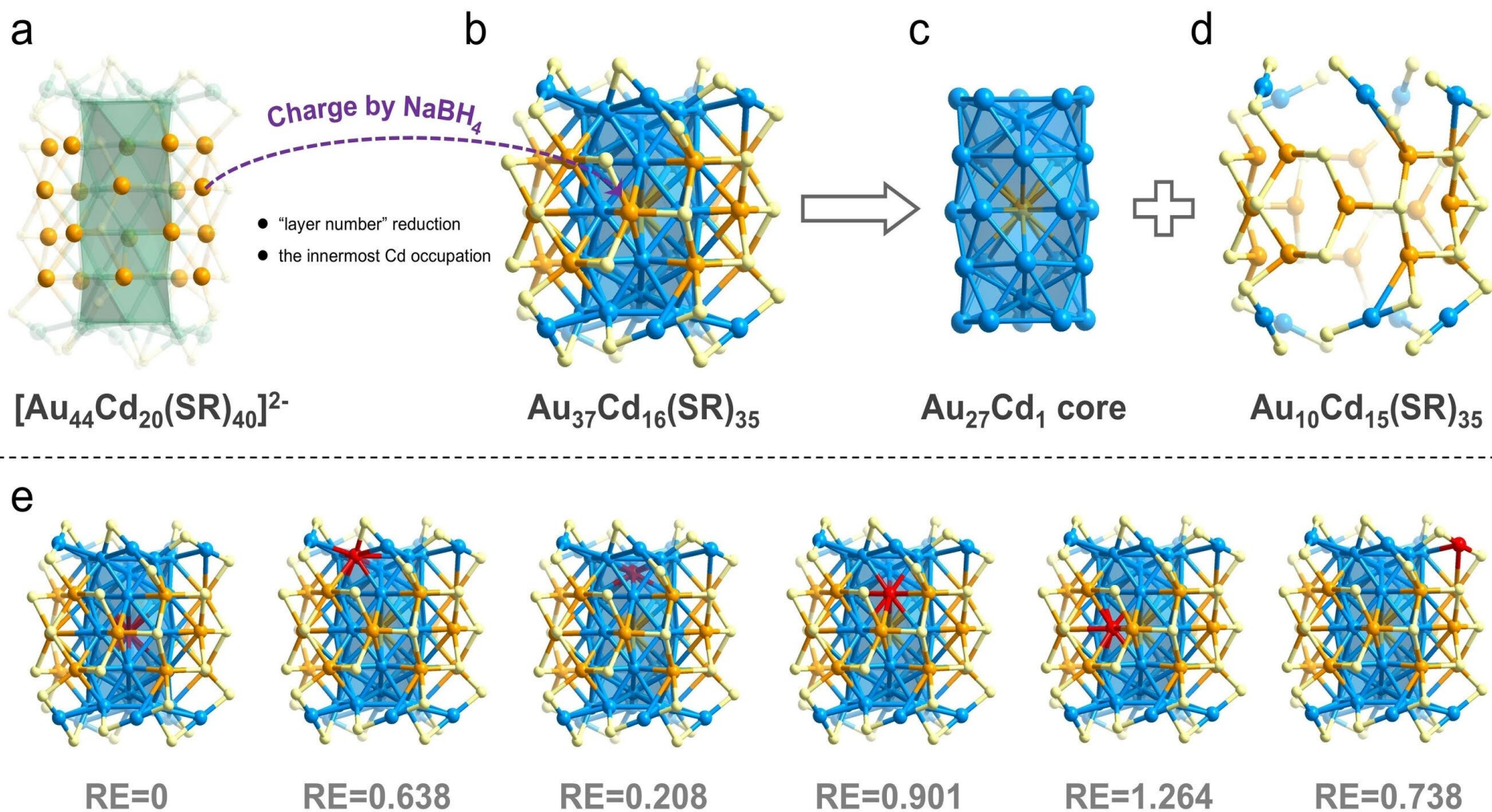


**Figure 3.** Structure anatomy and theoretical calculation of  $\text{Au}_{37}\text{Cd}_{16}$ . (a) Crystal structure of  $\text{Au}_{44}\text{Cd}_{20}$ . (b) Crystal structure of  $\text{Au}_{37}\text{Cd}_{16}$ . (c) Structure of the  $\text{Au}_{27}\text{Cd}_1$  core. (d) Structure of the  $\text{Au}_{10}\text{Cd}_{15}(\text{SR})_{35}$  staple. (e) Relative energy of  $\text{Au}_{37}\text{Cd}_{16}$  with different Cd occupations ( $\text{kcal mol}^{-1}$ ). For clarity, all carbon and hydrogen atoms are omitted. Cd: orange/red, S: yellow, and Au: other color.



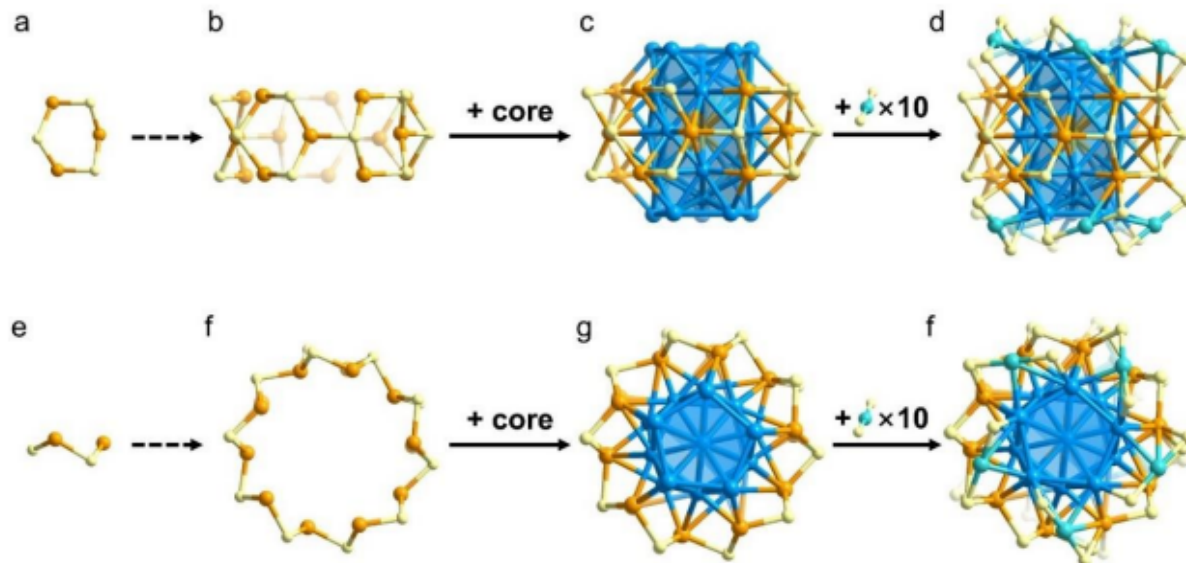


**Figure S9.** Anatomy of the structure of  $\text{Au}_{37}\text{Cd}_{16}$ . (a, e) Starting from the motif of  $\text{Cd}_3(\text{m-MBT})_3$ ; (b, f) the motif of  $\text{Cd}_{15}(\text{m-MBT})_{15}$ ; (c, g) adding the core to form the  $\text{Au}_{27}\text{Cd}_{16}(\text{m-MBT})_{15}$  framework; and (d, h) finally adding ten  $\text{Au}(\text{m-MBT})_2$  unit to form the complete structure of  $\text{Au}_{37}\text{Cd}_{16}(\text{m-MBT})_{35}$ . Side view: a-d; top view: e-h. For clarity, C and H atoms are all omitted. Cd, orange; S yellow; Au, other color.

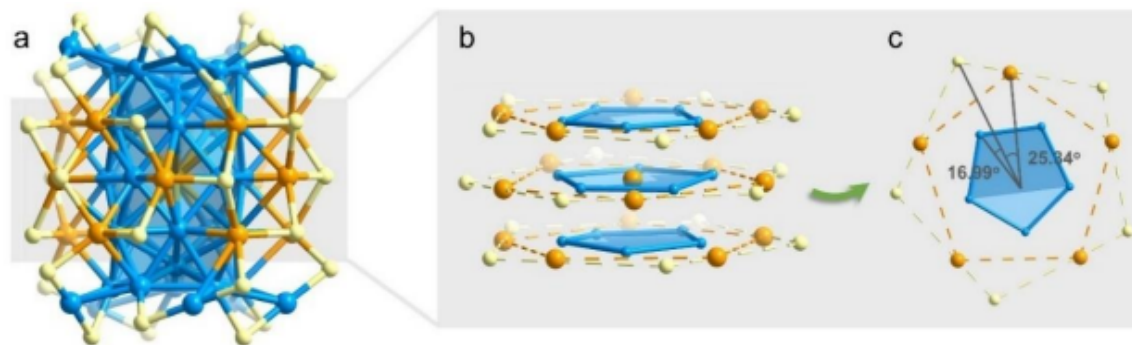


**Figure S10.** Layer by layer atomic arrangement of  $\text{Au}_{37}\text{Cd}_{16}$ . (a) Structure of  $\text{Au}_{37}\text{Cd}_{16}$ . (b) Illustration of  $\text{S}_5$ ,  $\text{Cd}_5$ , and  $\text{Au}_5$  pentagons in  $\text{Au}_{37}\text{Cd}_{16}$ . (c) Rotation relation between  $\text{S}_5$ ,  $\text{Cd}_5$  and  $\text{Au}_5$  pentagons in the same layer of  $\text{Au}_{37}\text{Cd}_{16}$ . For clarity, all C and H atoms are omitted. Cd, orange; S, yellow; Au, other color.

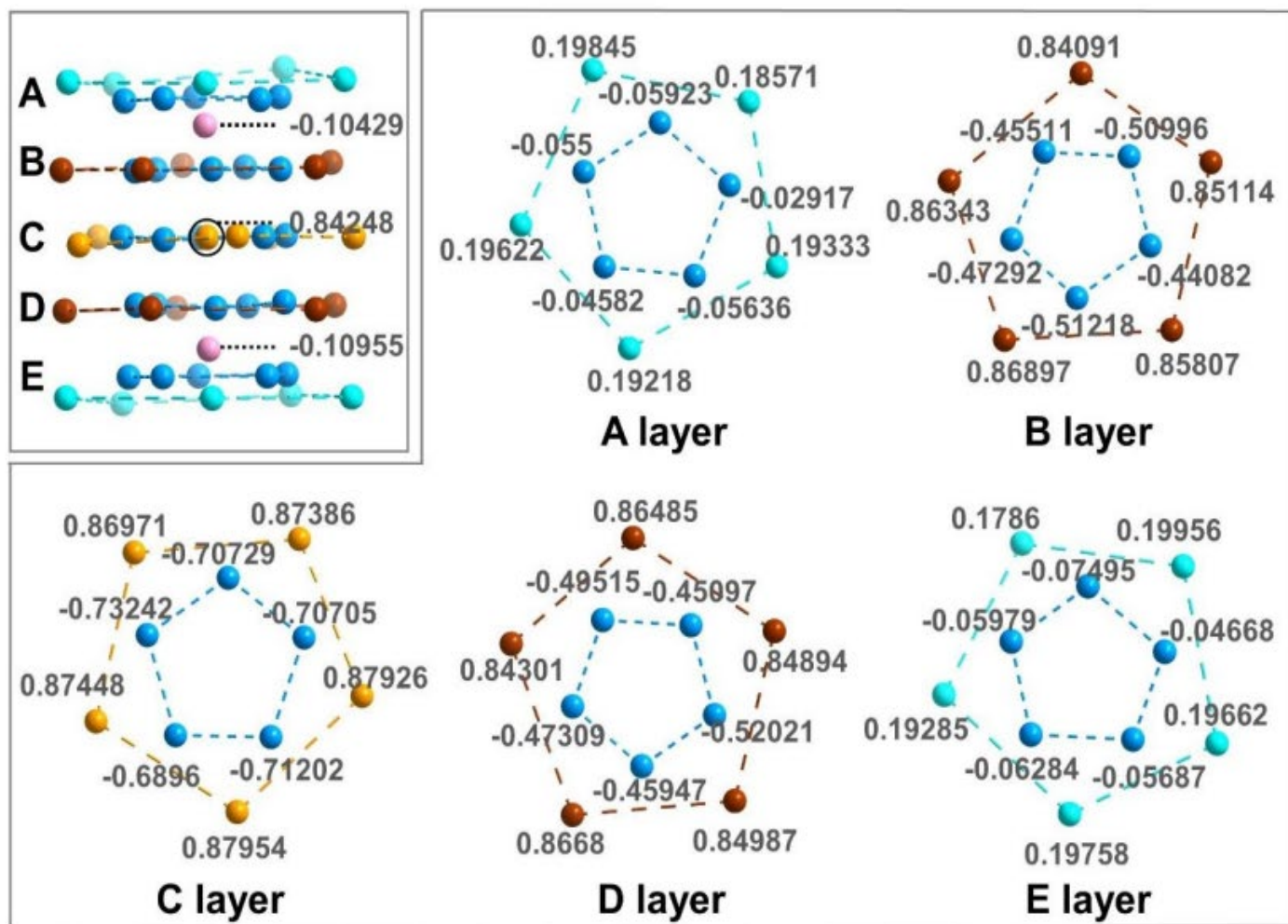


**Figure S28.** NPA Charge distribution of metal atoms in  $\text{Au}_{37}\text{Cd}_{16}$ . For clarity, all C and H atoms are omitted. Cd, orange/brown; Au, blue/pink/cyan.

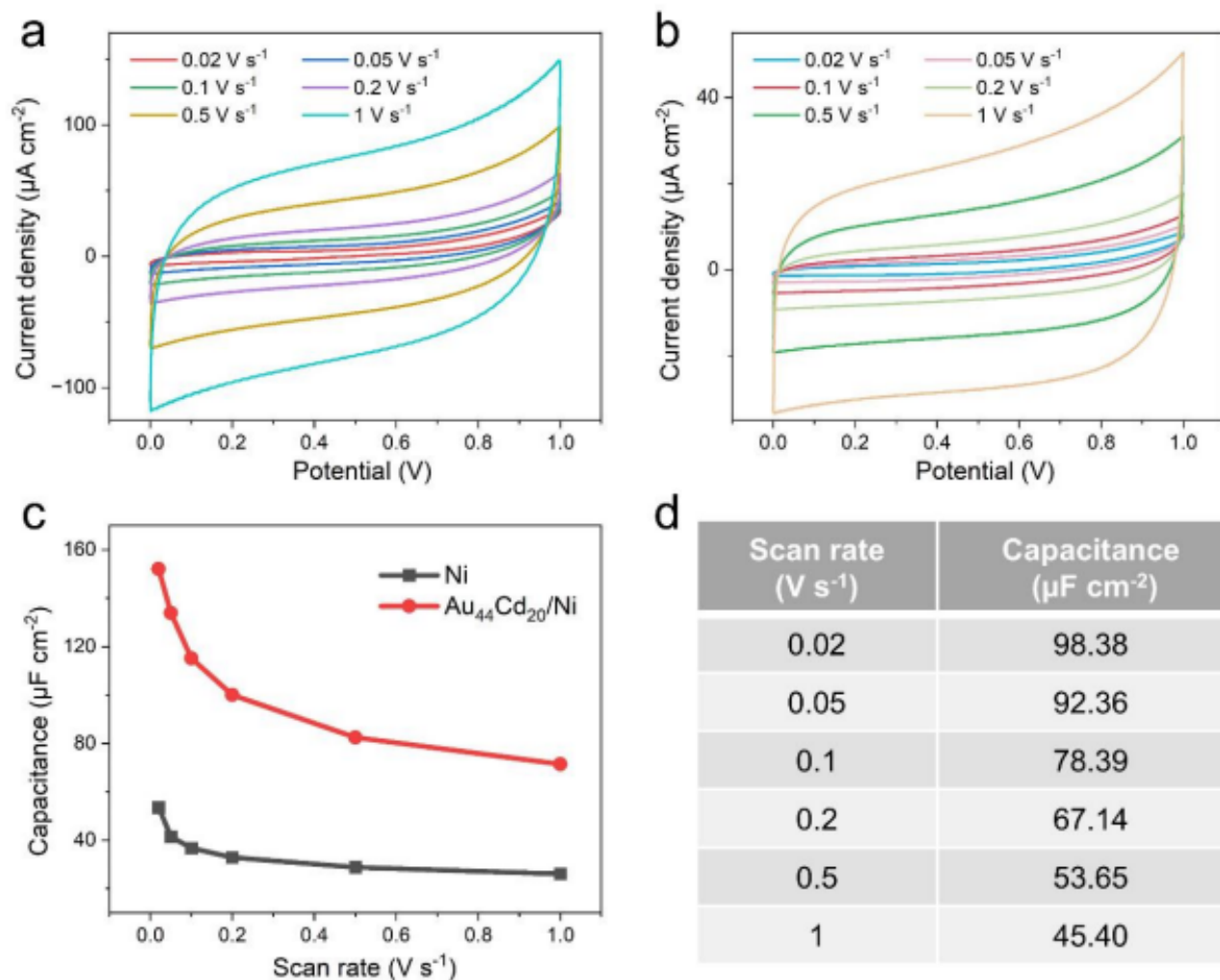


**Figure S16.** Cyclic voltammetry of Au<sub>44</sub>Cd<sub>20</sub>/Ni (a) and Ni (b) at various scan rates. (c) Capacitance comparison of Au<sub>44</sub>Cd<sub>20</sub>/Ni and Ni. (d) Summary table of Au<sub>44</sub>Cd<sub>20</sub> capacitances at various scan rates.

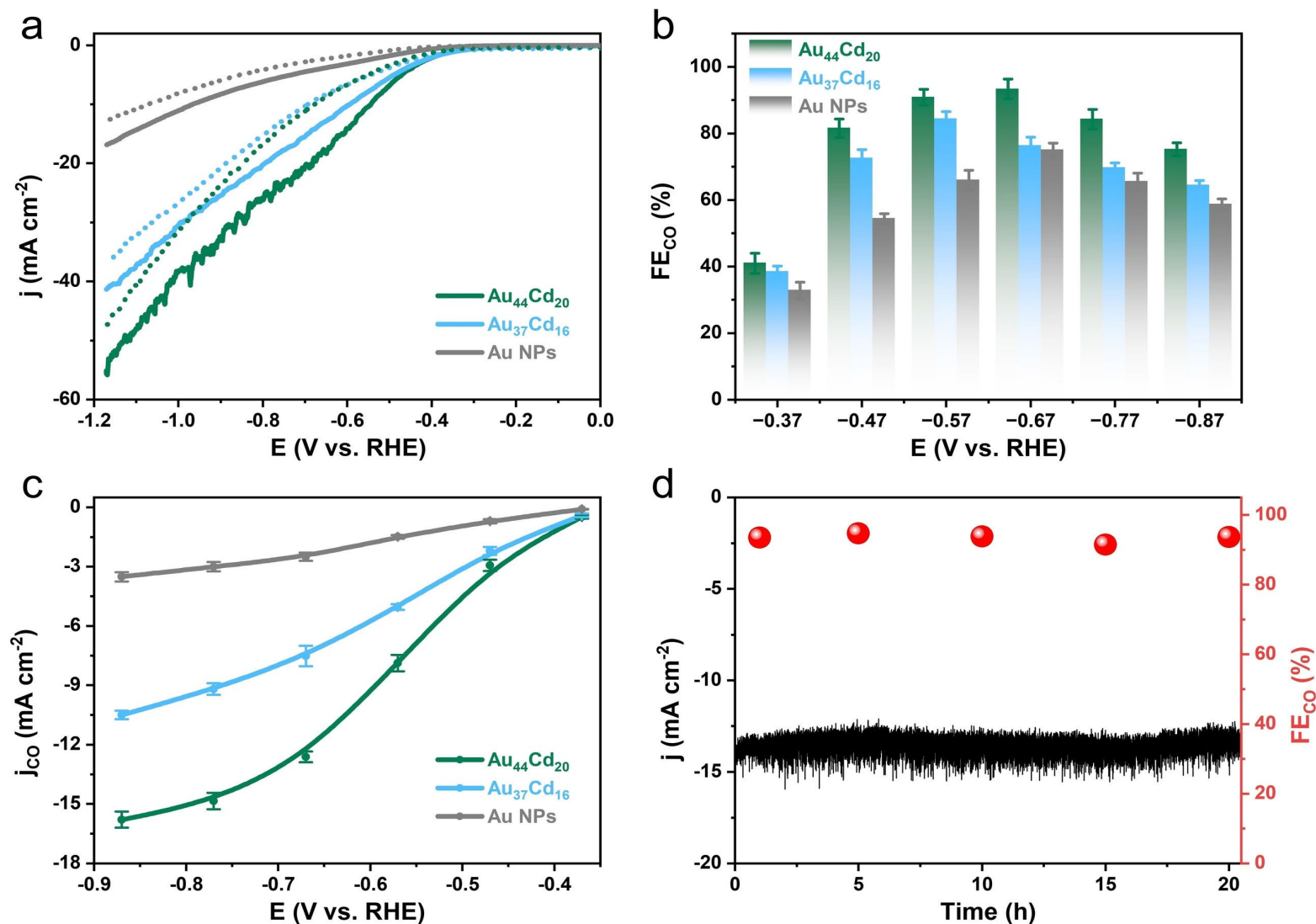


**Figure 4.** The electrochemical performance of Au<sub>44</sub>Cd<sub>20</sub>, Au<sub>37</sub>Cd<sub>16</sub> and Au NPs in 0.5 M KHCO<sub>3</sub>. (a) Linear sweep voltammetry curves in Ar-saturated (dotted line) and CO<sub>2</sub>-saturated (solid line) 0.5 M KHCO<sub>3</sub> solution with a scan rate of 10 mV s<sup>-1</sup>. (b) FE<sub>CO</sub> at different applied potentials. (c) The corresponding CO partial current density. (d) Electrocatalytic stability of Au<sub>44</sub>Cd<sub>20</sub> NCs for the electrocatalytic reduction of CO<sub>2</sub> to CO at -0.67 V for 20 h.



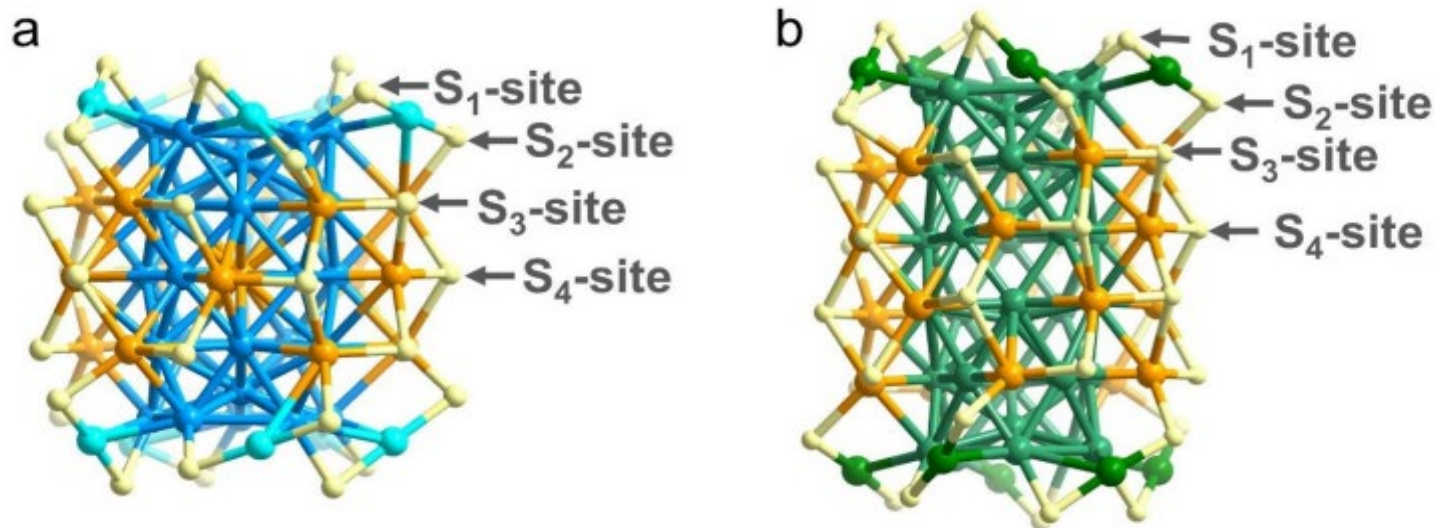


**Figure S21.** The calculated sites. (a)  $\text{Au}_{37}\text{Cd}_{16}$ . (b)  $\text{Au}_{44}\text{Cd}_{20}$ . For clarity, all C and H atoms are omitted. Cd, orange; S, yellow; Au, other color.

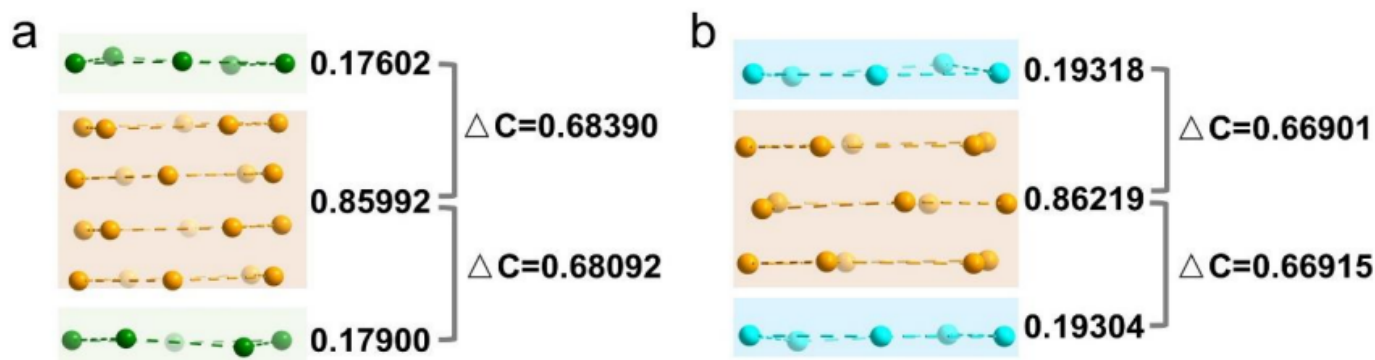


**Figure S30.** Comparisons of NPA charge difference ( $\Delta C$ ) between the Cd and Au sections. (a)  $\text{Au}_{44}\text{Cd}_{20}$ . (b)  $\text{Au}_{37}\text{Cd}_{16}$ . For clarity, all C and H atoms are omitted. Cd, orange; Au, magenta/green.

# Conclusion

- Reported a multilevel capacitor-like character of a novel  $\text{Au}_{44}\text{Cd}_{20}$  nanocluster
- NPA charge calculations show that average charges of the outer Cd shell and internal sleeve were 0.85992 and -0.39653, respectively, supporting the capacitor-like character
- This was further supported by voltammetry and the charge carrier transport in  $\text{Au}_{44}\text{Cd}_{20}$
- The charge carrier Cd(II) was transported from the middle shell to the innermost core with some structure modifications of  $\text{Au}_{44}\text{Cd}_{20}$  after charged by  $\text{NaBH}_4$  forming  $\text{Au}_{37}\text{Cd}_{16}$  without affecting the basal cannula structure
- The valence state of Cd changed from  $\sim +2$  to  $\sim 0$  during the charge carrier transport, indicating the occurrence of an intra-NC anti-galvanic reduction, which was not previously reported
- The  $\text{Au}_{44}\text{Cd}_{20}$  shell can be regarded as a subsidiary capacitor comprising the segregated Au and Cd sections, supported by the NPA charge and electrocatalytic  $\text{CO}_2\text{RR}$